

# Feasibility Study of Single-Photon Counting Using a Fine-mesh Phototube for an Aerogel Readout \*

R. Enomoto<sup>†</sup>, T. Sumiyoshi, K. Hayashi, I. Adachi

*National Laboratory for High Energy Physics, KEK, 1-1 Oho, Tsukuba-city, Ibaraki, 305 Japan*

S. Suzuki, H. Suzuki

*Hamamatsu Photonics K. K., 314-5, Shimokanzo, Toyooka Vill., Iwata-gun, Shizuoka, 438-01 Japan*

## Abstract

The fine-mesh phototube is one type of photodetector which can be used under a strong magnetic field. For an aerogel readout, the single-photon detection efficiency should be close to 100% in order to identify particle species. We carried out a feasibility study of single-photon counting using fine-mesh phototubes, and obtained a possible solution.

## 1 Introduction

Experimental high-energy physics in recent years has seen an increased demand for highly efficient photodetectors that can operate under a strong magnetic field. This is particularly true for the read-out of aerogel Cerenkov counters (Aerogel) [1] and ring-imaging Cerenkov detectors (RICH) [2]. Among other photo-detection devices, such as microchannel plate phototubes (MCP) and solid state detectors at low temperature, fine-mesh phototubes (FM) [3] seem to be the most promising due to their detection area, high quantum efficiency, radiation hardness, and stability. An FM phototube may also be used as the basis of a position-sensitive photon detection device by using segmented anodes (multi-anode phototube, MAPT) [4]. In this paper we present our feasibility study of FM phototubes used for single-photon detection. Our main interest is in its application to a charged-particle identification system based on aerogel Cerenkov counters. The results of our simulation and experimental studies concerning this area are presented.

## 2 Requirement for an Aerogel Readout

The motivation of our study was to develop a charged-particle ( $\pi/K$ ) identification system for a future B-factory experiment [5]. In an  $e^+e^-$  collision at  $\Upsilon_{4s}$ , a good  $\pi/K$  separation capability up to momenta of 3-4 GeV is required. Threshold-type aerogel Cerenkov counters (reflective index:  $n=1.02 - 1.006$ ) can be used for this purpose [6]. In this case, the typical number of Cerenkov photons produced by a relativistic pion above the Cerenkov threshold is not very large, about 4-5 [1]. A kaon is identified by detecting a charged particle associated with no corresponding Cerenkov photons. It is thus critical to employ a photon detection device with a high single-photon detection efficiency. Another important consideration is that the detector system must operate in a strong magnetic field, typically 1-Tesla, which is used for charged-particle momentum analysis in the experimental facility [5].

\*published in Nucl. Instr. Method **A 332** (1993) 129.

<sup>†</sup>internet address: enomoto@kekvax.kek.jp.

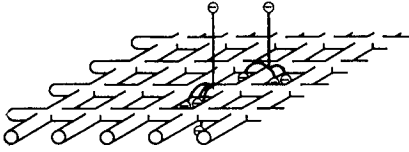


Figure 1: Basic configuration of a fine-mesh dynode.

### 3 Fine-mesh Phototube

#### 3.1 General

The fine-mesh (FM) phototube which we tested was developed by Hamamatsu Photonics K. K. (R2490-05, assembly-type H2611) [3]. Its outer diameter is 2 inches and the sensitive area comprises a 36-mm $\phi$  bialkali photocathode. The number of fine-mesh dynode stages is 16. The gap between neighboring dynodes is approximately 1.0 mm; that between the photocathode and the first dynodes is less than 3 mm. A typical gain is  $\sim 10^7$  ( at 2500V) without any magnetic field. Under a 1-Tesla axial field, the gain drops by 1/30 [3]. The phototube can be used within an inclination angle of 45 degree with respect to the magnetic field axis [3]. This phototube also shows a good transit time spread of 400 psec [7].

#### 3.2 Fine-mesh Dynodes

A basic configuration of the fine-mesh is shown in Fig 1. In total, the opacity is optically approximately 50%. The photocathode and dynodes are placed perpendicular to the phototube axis, so that the electrostatic field is almost axial. We therefore can not expect a much higher hit probability at the first dynode than the optical opacity. It is quite difficult to improve the hit probability of photoelectrons at the first dynode using this kind of phototube.

## 4 Single Photon Counting by H2611

Fig 2 shows a schematic view of the setup of our single-photon counting experiment. The incident photons are created by a thin (500 $\mu$ m) scintillator (NE101) illuminated by a  $\beta$ -ray source ( $^{90}\text{Sr}$ ). The trigger signal is created by a coincidence signal from two scintillators located downstream of this light source. To control the photon yield, approximately one photon per trigger, a collimator is used between the light source scintillator and the phototube to be tested. The pulse height of the phototube signal is digitized by a LeCroy 2249W ADC [8].

A calibration was carried out using the R3241 (Hamamatsu Photonics; GaAs-P first dynode); the measured pulse-height spectrum is shown in Fig 3-(a). A fit with a Poisson distribution gave the mean photoelectron yield:  $\mu=1.2$  per event. After this calibration, we carried out a test using the H2611 (Assembly of R2490-05: FM phototube). The pulse-height spectrum obtained by this FM phototube is shown in Fig 3-(b). The high voltage was adjusted to have a total gain of  $6 \times 10^7$ . Thus, the expected ADC count for a single photon was considered to be 137 channel (ch.), where the pedestal was 97 ch. Although a clear dip structure at around 120-ADC counts was seen in the data, we could not obtain a clear peak that was consistent with the Poisson distribution. In the following section we examine the observed signal pulse-height structure.

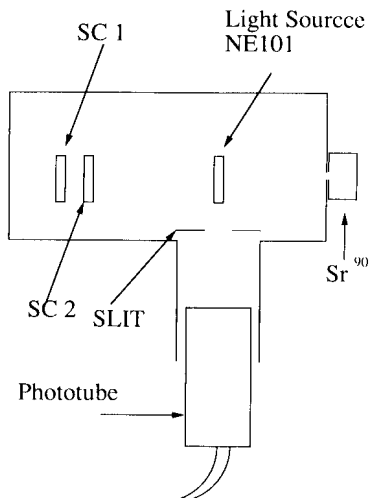


Figure 2: Experimental setup for single-photon counting.

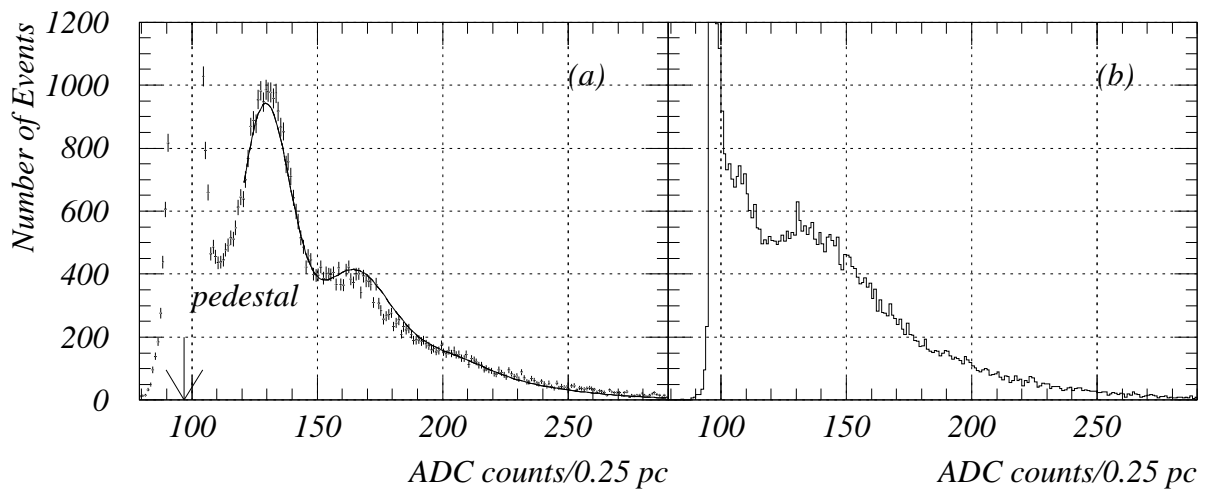


Figure 3: Pulse-height spectra obtained by the test: (a) for R3241, and (b) for H2611 (FM phototube). In (a), a best-fitted Poisson function is plotted (curve). The pedestals for these plots were 97 ch.

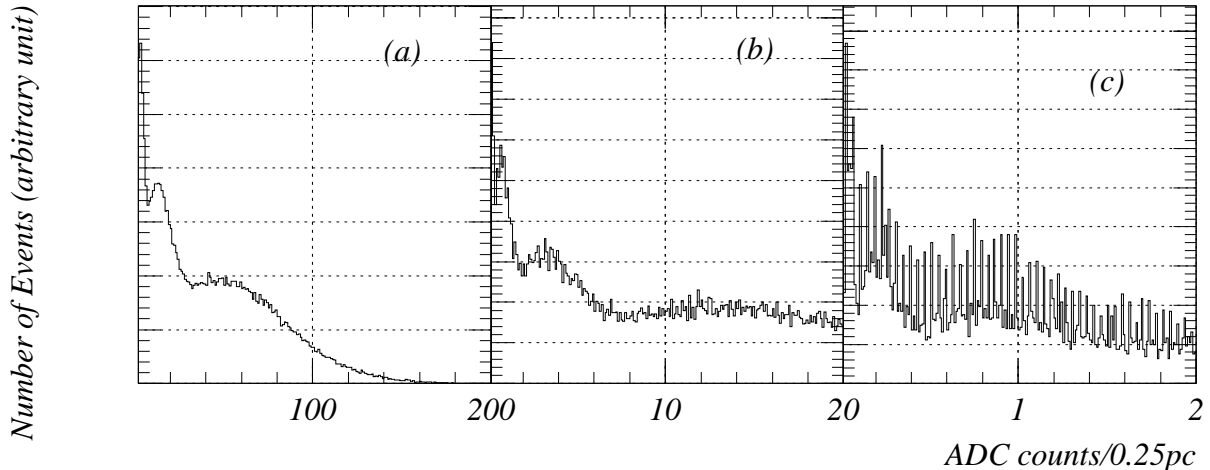


Figure 4: Pulse-height distribution obtained by a simulation of single-photoelectron events: (a) ADC range 0-200, (b) ADC range 0-20, and (c) ADC range 0-2.

## 5 Simulation Study

### 5.1 Simple Simulation

At first, we started by making a simple assumption: that the hit probability of electrons on each dynode was 60%. The total gain of phototube was assumed to be  $2.5 \times 10^7$  by 12 dynodes, while each dynode gain was assumed to be equal. A single photoelectron was generated at the photocathode and the number of secondary electrons at each dynode was randomly created according to Poisson distributions. The resulting pulse-height distributions are shown in Figs 4-(a),(b), and (c) with three different horizontal bin sizes. Accidentally, the pulse-height distribution of Fig 4-(a) coincided with Fig 3-(b) by the FM phototube. It is shown that single-photon events would not emerge as a clear peak but, rather, they create a fractal-structure in the pulse height spectrum.

A fractal structure appears when a process is described in terms of the function  $x^\alpha$  [9]. In the FM phototube case,  $x$  is the dynode gain and  $\alpha$  is the effective number of dynodes, i.e., the dynode hit probability times the number of dynodes;  $\alpha$  is typically a noninteger. The pulse-height distribution should therefore have a similar shape in any ADC range; it is thus impossible to obtain the peak structure. The peak around 130-ADC counts shown in Fig 4-(a) is considered to be the case in which a photoelectron hits the first dynode; the peak around 110-ADC count is for a photoelectron hitting the second dynode. The pulse-height difference between two peaks is the same as the dynode gain, and the ratio of each peak entry is same as the dynode hit probability. Thus, it is again understood that a single-photon peak cannot be observed by FM phototubes, even by increasing the first dynode gain or by improving the first dynode hit probability. Even upon setting a low threshold, an inefficiency remains.

### 5.2 Possibility of Single-Photon Counting

In order to cure this situation,

1. obtaining a higher gain, and/or
2. making the pulse height distribution harder

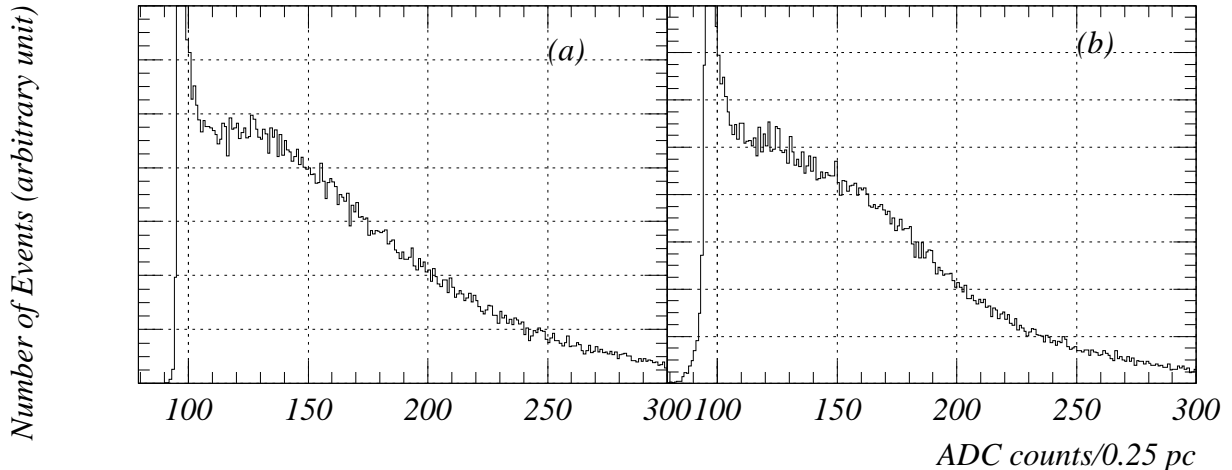


Figure 5: Single-photon spectra obtained by the improved phototubes: (a) H2611(19) and H2611(24).

are necessary. Both situations can be realized by increasing the number of dynodes. By this method, each dynode gain can be reduced and the gap between peaks can be made smaller. Events which started multiplication at deeper dynodes can thus be saved.

Using the same simulation we increased the number of dynodes to 15 and 20. The pulse-height distributions became harder. In addition the waving structure disappeared due to the low gain of each dynode.

In order to make a single-photon peak, we must significantly increase the probability of the first dynode hit. We checked this using the same simulation and concluded that a probability greater than 90% is necessary. If we provide such a high opacity in fine-mesh dynodes, secondary electrons cannot be transported to the second dynode. Therefore, we may need other kinds of dynode structures, for example wire dynodes (grids) with an alternating high voltages to produce a highly focused electric field.

## 6 Improvement of the Fine-mesh Phototube

According to the results obtained by the simulation, we developed phototubes with a larger number of dynodes, i.e., 19-dynodes (H2611(19)) and 24 dynodes (H2611(24)). The former one was made using the same type of glass tube as that used for the R2490-05 phototube; for the latter, a longer glass tube was made.

The typical gains at 2500V obtained by these phototubes without any magnetic field were  $6 \times 10^7$  and  $1.2 \times 10^9$  for H2611(19) and H2611(24), respectively. There was no increases in the dark current due to these improvements.

## 7 Experimental Study

### 7.1 Experimental Results

We carried out tests using the setup shown in Fig 2. The single-photon spectra obtained by these two phototubes are shown in Figs 5-(a) and (b) for H2611(19) and H2611(24), respectively. The high voltages

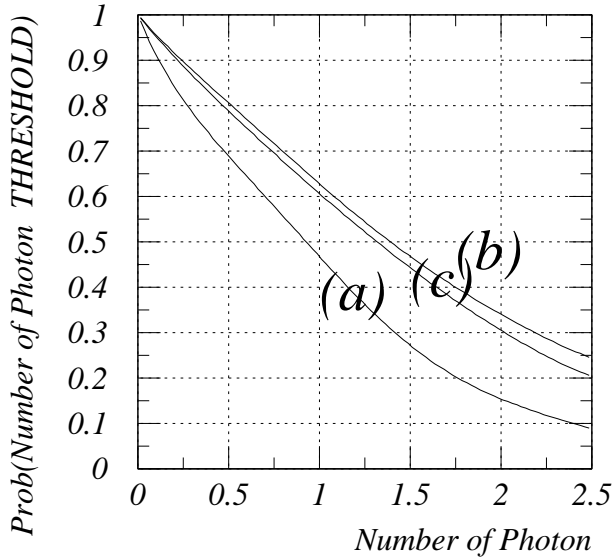


Figure 6: Single-photon efficiencies versus threshold values: (a) for H2611, (b) for H2611(19), and H2611(24).

were adjusted so as to obtain gains of  $6 \times 10^7$  in both cases. The single-photon efficiencies were consistent with that of the H2611 (Fig 3) at the extrapolation to a zero-threshold. The waving structure disappeared and the spectrum shapes became harder, as expected, due to the previously described simulation.

We tried to obtain relations of the single-photon efficiencies versus the threshold values by the following method. We derived the relationship between the integrated contents, which were greater than the threshold values, versus the thresholds. The normalizations were carried out using polynomial-fits to these relationships at zero-threshold points. The results for three kinds of phototubes are given in Fig 6. There was a clear improvement of H2611(19) compared to that of H2611. The results of H2611(19) and H2611(24) were similar to each other within the experimental errors (including the statistical and systematic errors). In order to obtain the single-photon efficiency greater than 90%, we must lower the thresholds to 0.1-photon for the H2611 and 0.25-photon for the improved phototubes; this was quite easy for the improved tubes owing to the high gain. In case of the H2611, it was suggested that use of a preamplifier under low-gain operation would yield a high efficiency. Using the simulation described so far, the suggested gain was less than  $10^6$ .

## 7.2 Test under Magnetic Field

The gain and single-photon measurements were carried out under a 1 tesla magnetic field. The phototube used in these tests was the H2611(24). Fig 7 shows the angle dependence of the phototube gain. The vertical scale is the gain at an inclination angle with respect to the magnetic field axis normalized by the gain at  $B=0$ . The angle dependence of the gain was similar to the case of the H2611(16), except for the overall scale factor. The gain drop observed for the H2611(24) was about 1/50 at 0 degree, larger than that of the H2611(16) ( $\sim 1/30$ ). It is therefore hard to read it out without using a preamplifier. The high-voltage dependence of the gain was also measured. The gain was typically described by the function  $V^\alpha$ ; we could not observe any magnetic field dependence of  $\alpha$ .

The single-photon spectrum was measured at 1 tesla with an inclination angle of 15 degrees (Fig 8). In this case we used a preamplifier because of the low gain. The light source was a pico-second laser; a histogram was obtained by self-triggering. The histogram shown in Fig 8 is a background-subtracted type

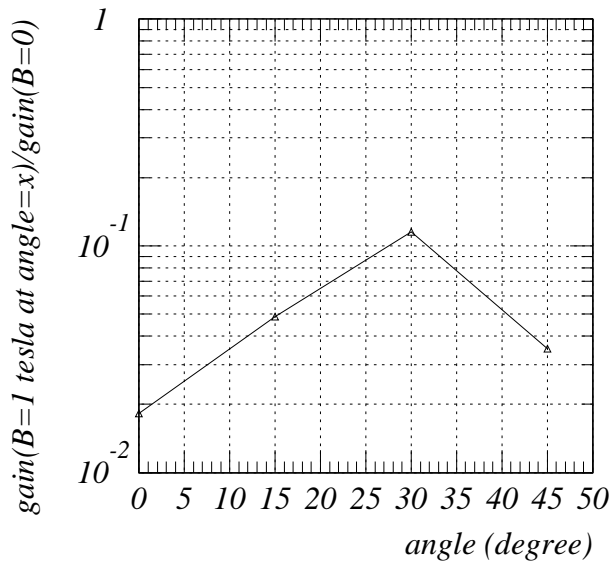


Figure 7: Gain under a 1 tesla magnetic field. The horizontal axis is the inclination angle with respect to the magnetic field axis. The vertical scale is the normalized gain with respect to the gain without a magnetic field.

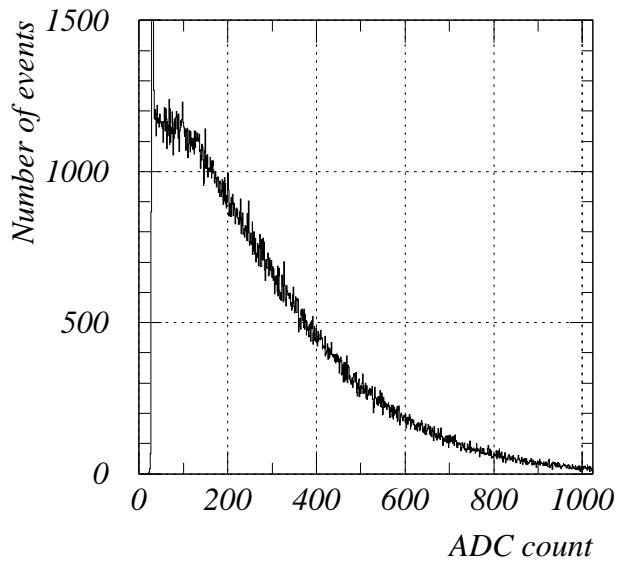


Figure 8: Single-photon spectrum by the H2611(24) at 1 tesla with an inclination angle of 15 degrees.

(i.e. on-source minus off-source run). The single-photon spectrum was similar to Fig 5 (b). Therefore, single-photon detection under a magnetic field was proven.

## 8 Summary

We carried out systematic studies on single-photon counting using fine-mesh phototubes, especially for the purpose of aerogel readouts. The studies were carried out using both simulations and experiments. We found one possible solution to improve the single-photon efficiency: to increase the number of fine-mesh dynodes. We concluded that fine-mesh phototubes can be used for an aerogel Cerenkov counter readout at a future B-factory.

## Acknowledgement

We appreciate the support given by Prof. H. Sugawara, Prof. S. Iwata, Prof. M. Kobayashi, and Prof. F. Takasaki in carrying out this R and D. We also thank Prof. F. Takasaki and Prof N. Toge for their valuable discussions. We greatly appreciate the technical staff of KEK and Hamamatsu Photonics K. K.

## References

- [1] A. Onuchin et al., to be published in Nucl. Instr. Meth. **A 315** (1992) 517.
- [2] J. Seguinot, CERN-EP/89-02, July (1989).
- [3] A. Sawaki et al., IEEE Trans. Nucl. Sci., **NS-31**, **1** (1984) 442; M. D. Rousseau et al., IEEE Trans. Nucl. Sci., **NS-30**, **1** (1983) 479; H. Kume et al., IEEE Trans. Nucl. Sci., **NS-32**, **1** (1985) 355; S. Suzuki et al., IEEE Trans. Nucl. Sci., **NS-33**, **1** (1986) 377.
- [4] F. Takasaki et al., Nucl. Instr. Meth., **A 260** (1987) 447.
- [5] Proceedings of “Physics and detectors for KEK asymmetric B factory”, KEK Proc 91-07, KEK, Tsukuba, Japan (1991).
- [6] P. A. Coyle et al., SLAC-PUB-5594, Sep. (1991).
- [7] B. Lekovar et al., Nucl. Instr. Meth., **A123** (1975) 145; F. Takasaki et a., Nucl. Instr. Meth., **A228** (1985) 369.
- [8] See Nuclear Products Summary, LeCroy.
- [9] H. Takayasu, “Fractal in the physical science”, Manchester Univ. Press (1990) 157.